Journal of King Saud University – Science 35 (2023) 102804

Contents lists available at ScienceDirect

Journal of King Saud University – Science

journal homepage: www.sciencedirect.com

Original article

Regional distribution of intensity–duration–frequency (IDF) relationships in Sultanate of Oman

Prerana Chitrakar [a], Ahmad Sana [a,*], Sheikha Hamood Nasser Almalki [b]

[a] Department of Civil and Architectural Engineering, Sultan Qaboos University, P.O. Box 33, Al-Khoudh 123, Oman
[b] Aflaj Inscribed in World Heritage List, Ministry of Agriculture, Fisheries Wealth and Water Resources, Muscat, Oman

ARTICLE INFO

Article history:
Received 20 September 2022
Revised 10 January 2023
Accepted 13 July 2023
Available online 20 July 2023

Keywords:
Regional IDF curves
Rainfall data analysis
Gumbel distribution
Ungauged catchments

ABSTRACT

Analysis of extreme rainfall parameters including rainfall intensities is a fundamental requisite in safe planning, designing, and operating various hydrologic and water engineering projects against storms and floods. In arid and semi-arid regions, such as Oman, sufficient long-term rainfall data with short aggregation are usually not available in most locations across the country. This paper presents the development of intensity duration frequency (IDF) curves using the available rainfall data from 65 meteorological stations situated at different elevations and regions throughout Oman. Gumbel distribution was fitted to the observed data and rainfall intensities were found for various return periods. Rainfall analysis showed the average annual rainfall of 109.21 mm with a standard deviation of 92.82 mm, Skewness coefficient of 1.62 and Kurtosis coefficient of 3.08 for all the studied stations from 1977 to 2017. The statistical analysis showed that the estimated rainfall intensities for various return periods are high in the mountainous region compared to the desert or interior region, and the coastal region of the country. Also, the empirical parameters of IDF formula for all studied stations were established using non-linear regression. Finally, the contour maps for all the parameters were drawn which could be used to determine the IDF relationships for ungauged locations. This study will be useful for the decision makers and practicing hydrologists for planning and design of water resources systems in Oman.

1. Introduction

Rainfall is a fundamental constituent of the hydrological cycle. Consequently, the determination of rainfall events is important for planning and designing of any hydrologic project including storm and drainage designs, geotechnical and structural projects, water resources systems, and others. However, the development of any hydrological project is highly challenging in the arid region where the rainfall is largely random and erratic both temporally and spatially (Al-Amri and Subyan, 2017). The changes in precipitation as the result of extreme weather events in the water-scarce arid countries is often facing long-term droughts and flash floods; damaging coastal, residential and agricultural areas and natural habitats in the arid region (Cosgrove and Loucks, 2015; Gunawardhana and Al-Rawas, 2016). The recent climate change is considered as one of the major challenges for water supply systems and flood risk analysis works (Ishak et al., 2013; Kourtis and Tsihrintzis, 2022). Thus, the quantification of rainfall is performed using intensity–duration–frequency (IDF) curve (Chow et al., 1988) as a tool, to implicate safe design and cost efficiency to the hydrologic and engineering projects for certain return period (Raiford et al., 2007). The site specific IDF is used to study the relationship between rainfall intensity, duration and frequency (or return period) associated with the site location and amenities (Chow et al., 1988).

The IDF relationship was first presented by Bernard (1932). Since then, different forms of IDF relationships have been established by many researchers in the field of engineering, hydrology and environmental studies in several regions of the world. IDF formula was developed by Bell (1969) and Chen (1983) for few regions of United State. Koutsoyiannis et al. (1998) constructed the mathematical framework of IDF curve using data from both rainfall recording and non-recording stations based on probability distribution. But, the probability distributions are considered as

* Corresponding author.
E-mail addresses: P.Chitrakar@squ.edu.om, Prerana_22@hotmail.com (P. Chitrakar), sana@squ.edu.om, sana092@yahoo.com (A. Sana).

Peer review under responsibility of King Saud University.

Production and hosting by Elsevier

https://doi.org/10.1016/j.jksus.2023.102804

stationary and do not change with time (Vinnarasi and Dhanya, 2022). Whereas, the climate change is likely to alter the climatic extremes over the time, given the stationary IDF curve approach often underestimates the precipitation extremes (Cheng and AghaKouchak, 2014; Shrestha et al., 2017). Several studies using non stationary model using climate indices as covariates were explored in few studies (Li et al., 2015; Bracken et al., 2018; Silva et al., 2021; Vinnarasi and Dhanya, 2022). Raiford et al. (2007) updated the existing IDF curves for the different region of United States; and, acquired those curves at ungauged sites throughout the region using the newly developed rainfall frequency analysis methods. El-Sayed (2011) used *iso*-pluvial maps in Egypt; Awadallah et al (2011) used regional analysis and satellite data in Angola; Yu et al. (2004) used scaling theory in Taiwan; Ouali and Cannon (2018) used quantile regression technique in Canada for developing the regional IDF at the ungauged sites. Likewise, Noor (2022) proposed method for IDF curve construction with related uncertainty at the ungauged sites using bias correction of satellite rainfall data and its comparison with the observed IDF Curve.

Several researchers have developed the IDF curve for the arid Arabian Peninsula using both empirical formulae and frequency analysis. Various theoretical distribution functions (Generalized Extreme Values (GEV), Gumbel distribution, Generalized Pareto Distribution (GPD), Log Pearson Type III, Log Normal, Exponential distribution and others are normally used in frequency analysis (Sherif et al., 2014; Forestieri et al., 2018; M. Bermúdez et al., 2020). Al Shaikh (1985), and Al Areeq et al. (2021) used Gumbel distribution for development of IDF curve in various region of Saudi Arabia. Elsebaie (2012), Al-Amir and Subyan (2017) used both Gumbel and Log Pearson III distribution; while, AlHassoun (2011), (Al-anazi and El-Sebaie, 2013) used Gumbel, Log Pearson III, and Log Normal distribution for development of IDF curve in several locations of Saudi Arabia. There studies did not show much difference in the rainfall analysis of IDF curve for Gumbel and Log Pearson Type III distribution for the semiarid and flat topographic region.

The development of IDF relationship requires the long-term and continuous historical rainfall data, which is typically not available in most semiarid and arid region countries including Sultanate of Oman. Also, the precipitation events in the region are rare but usually of high intensities in the short duration, resulting in flash floods in an inter-annual scale (Uraba et al., 2019; Aldosari et al., 2020). Precipitation frequency analysis is equally important in nonstructural problems concerning natural risks related with ultimate rainfall events (Maidment, 1993). The data required to compute IDF curves are a record of rainfall depth measurements during fixed intervals of time, normally 5 min intervals (Mays, 2005). Thus, the coarse-resolution precipitation data is converted into the fine time-resolution precipitation using the temporal disaggregation technique (Al-Wagdany, 2021).

Very limited studies in rainfall analysis and climate change projection has been conducted for Oman. Awadallah (2017) designed a storm hyetograph of few stations located at the Northern coastal zone of Oman using Alternating Block Method (ABM)-IDF Curve method. While, Uraba (2019) has developed the IDF curve for Tawi-Atair station in Dhofar region of Southern Oman using two-stage downscaling disaggregation approach. Thus, the IDF relationships are not available for most of the regions in Oman. In the absence of a properly developed IDF relationship, the planning and development of water resources systems such as recharge dams, flood protection structures, storm water collection networks and other projects may result in improper design. Also, the developed IDF curves can be adopted to quantify the rainfall rate and predict the flooding for any region. Therefore, this research aims to develop IDF curves for the Oman, by analyzing rainfall data at multiple meteorological stations situated at different elevations and regions throughout the country using Gumbel distribution. The empirical formulae were also developed to evaluate rainfall intensity for several rainfall durations and return periods. Further, the contour maps for all the observed parameters were drawn to establish the IDF relationships for the ungauged location for future predictions and designs.

2. Study area and data collection

Oman (Sultanate of Oman) lies in the southeastern corner of the Arabian Peninsula with total area of 309,500 km^2 and a coastline 3165 km long. It extends between latitudes of 16°40′ and 26°20′ N and longitudes of 51°50′ and 59°40′ E. The country is bordered by Arabian Gulf in the North, Sea of Oman in the East, Arabian Sea in the Southwest, United Arab Emirates and Saudi Arabia in the West, and Yemen in the Southwest as shown in Fig. 1 (FMO, 2022). Topographically, it is divided into three areas; the coastal plain (fertile plain) extends from Al Batinah Plain in the North to Salalah Plain in South, mountainous region runs from Musandam in the North to Ras Al-Hadd in the Southeast and in Dhofar province, and the internal region (desert, gravel and sand plain) ranges from the coastal plain to the mountainous region covering 82% area of the country (FAO, 2021).

Based on rainfall, Oman experiences the hyper arid (less than100 mm rain), arid (100–250 mm rain) and semiarid (250–500 mm rain) climate at various parts of the country (Kwarteng et al., 2009). The long-term average annual rainfall of the country has been estimated to be 62 mm (MRMWR, 2013). Average annual rainfall in the desert and coastal plain is less than 50 mm; while the rainfall in mountain region is up to 350 mm, and is relatively frequent providing recharge to the aquifers situated at the coastal and interior plains (Al Barwani, 2014). Seasonal summer monsoon is observed from June to September in southern parts of the country, especially in Dhofar Governorate causing change in temperature. Whereas, the rainfall occurs during winter from November to April in the northern and central region of the country (FAO, 2021). In summer, the weather is hot and humid in the coastal region, hot and dry in interior region; while, the weather is moderate and rainy throughout the year in the highlands (FAO, 2021). Rainfall in the country is associated by four principal mechanism; convection rainstorms related with localized strong convection developed mostly in summer, cold front trough from Mediterranean Sea or North Atlantic that brings rainfall to northern part of Oman especially from November to April, tropical cyclones originated from Arabian Sea typically from May to June and October to November, and on-shore southwesterly monsoon current that causes humid environment and brings frequent drizzle, mist, fog, rain in Dhofar region from June to September (Roberts and Wright, 1993; MWR, 1995).

In this study, the rainfall data were obtained from the Ministry of Regional Municipalities and Water Resources (MRMWR). Oman is divided into eleven governates, namely; Musandam, Al-Buraimi, Al-Batinah North, Al Batinah South, Muscat, Adh Dhahirah, Ad-Dakhaliya, Al-Sharqia North, Ash-Sharqia South, Al-Wusta, and Dhofar. Sixty-five monitoring stations are selected to cover the ten governates in the country. Al Wusta govenerate, the desert area is not considered in the study due to lack of enough stations and data for analysis. The selected stations had homogenous and short time interval record for longer period. The record length varies from one station to another, which was because of some missing years of data and initial years of gauge installation at the sites. The record periods were between 20 years to 40 years of rainfall data. The location details and years of record of stations that were used for this study are shown in Table 1 and Fig. 1.

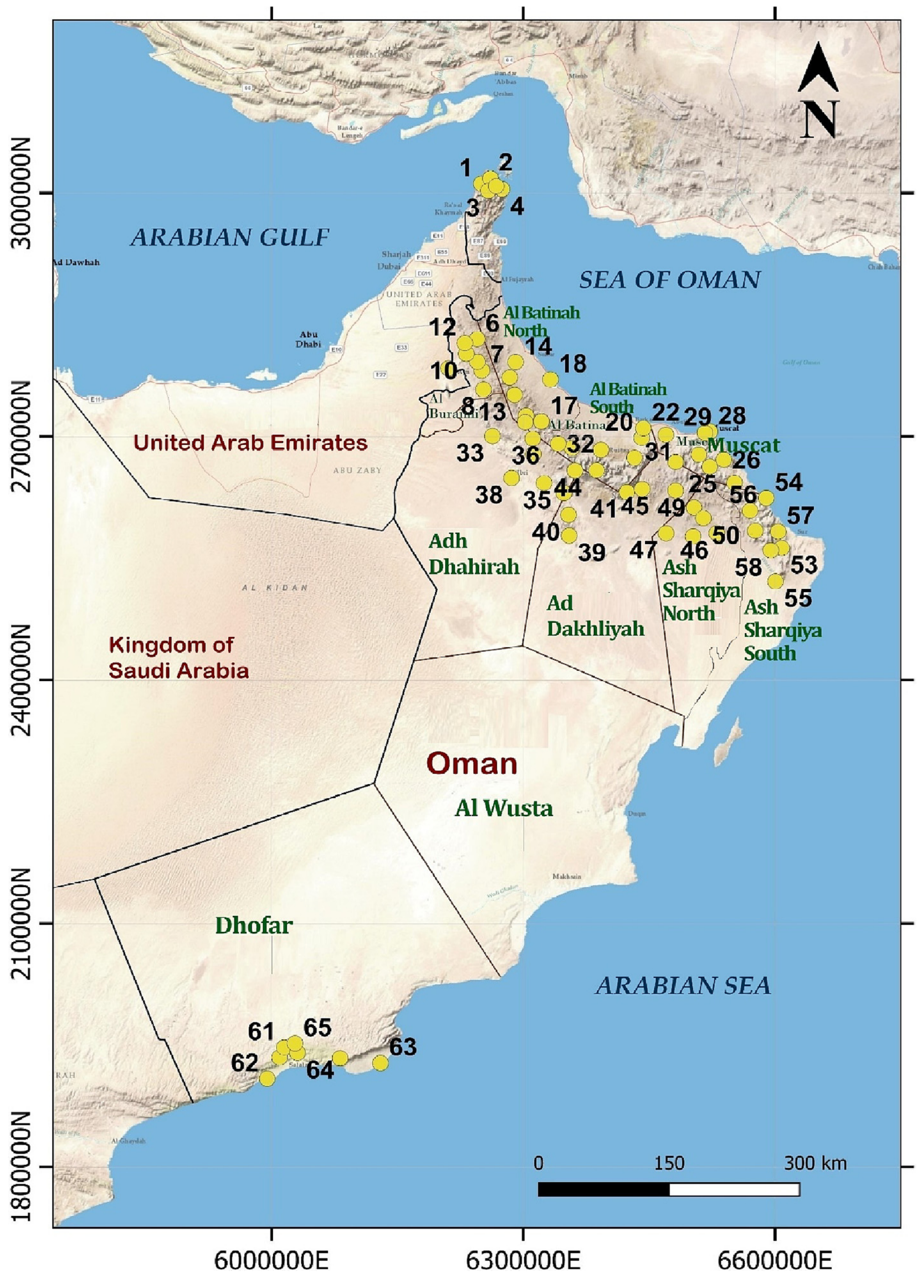

Fig. 1. Study Area with governorate and studied stations (FMO, 2022).

3. Methodology and data analysis

Estimation of IDF curves involved various steps. Initially the rainfall data were analyzed and disaggregated for the shorter period. Collected data from monitoring stations were initially sorted according to the years, rainfall depth and duration. Disaggregation of rainfall data to shorter and regular period was done using the Hydrologic Engineering Center's (HEC) Data Storage System Visual Utility Engine (HEC-DSSVue) software. Maximum rainfall depth is acquired for each monitored year and various durations. Statistical analysis such as mean and standard deviation of the maximum rainfall depth were also obtained for various durations.

Development of IDF is performed by fitting the probability distribution function to extreme rainfall data for specific durations. Based on measurements and fitted relationship, the rainfall intensity over specific duration and return period are determined for the recorded years. Gumbel distribution is used for frequency analysis of the annual maximum rainfall data for the calculation of rainfall depth for each return period. Design durations of 5, 15, 30, 60, 360, 720, 1440 min, and return periods of 2, 5, 10, 25, 50 and 100 years were used in the present study. Further, the parameters of the IDF relationship proposed by Bernard (1932) are obtained using regression. Finally, the contour maps for all the parameters were drawn using SURFER software for determining the IDF relationships for ungauged locations.

3.1. Gumbel distribution

Extreme value Type I (Gumbel) distribution, proposed by German mathematician Emil Gumbel (Gumbel, 1958) is widely used for modeling extreme events in the field of water resources engineering. The distribution had over 50 applications

Table 1
Station detail with year and length of rainfall records.

S.N.	Governorate	Station Name	Easting (m)	Northing (m)	Elevation (m)	Years of Record	Length of Records (Years)
1	Musandam	Ghamda	414,500	2,887,100	45	1981–2017	37
2		Khasab	424,300	2,892,800	37	1983–2017	35
3		Rhaibah	421,936	2,879,218	704	1986–2016	31
4		Sal Ala	436,466	2,880,987	171	1983–2016	34
5		Sima	430,384	2,884,322	129	1981–2017	37
6	Al Buraimi	Al Juwayf	408,900	2,715,000	634	1996–2016	21
7		AL Ubaylah	413,619	2,679,851	604	1997–2016	20
8		Fayyad	415,400	2,658,600	626	1995–2014	22
9		Khatwah	409,000	2,689,600	622	1995–2014	20
10		Mahdah	396,900	2,698,800	437	1985–2016	32
11		Wadi Salmah	377,500	2,682,700	300	1982–2017	36
12		Wadi Sharm	395,400	2,710,700	452	1989–2016	28
13	Al Batinah North	Al Ghuzayfah	449,210	2,652,513	510	1989–2017	29
14		Al Jizzi	450,426	2,689,150	167	1995–2016	22
15		Aqair Al Abreein	461,672	2,629,031	741	1997–2016	20
16		Aqbat Al Risah	444,008	2,671,956	516	1995–2017	23
17		Hayl Al Najd	478,400	2,622,600	922	1997–2016	20
18		Saham	488,292	2,669,695	12	1988–2016	29
19	Al Batinah South	Al Miseen	580,300	2,582,000	363	1993–2016	24
20		Al Wasit	588,000	2,604,500	118	1993–2016	24
21		Ar Rustaq	543,500	2,590,700	309	1991–2016	26
22		Barka	589,700	2,615,200	29	1988–2016	29
23		Dhabaah	511,800	2,592,900	916	1983–2016	34
24		Salma	538,700	2,567,700	1124	1992–2016	25
25	Muscat	Buei	662,700	2,572,500	433	1994–2016	23
26		Hayfadh	678,100	2,580,700	208	1995–2016	22
27		Mazara	690,200	2,554,900	130	1981–2016	36
28		Muscat	662,400	2,612,200	7	1992–2016	25
29		Ruwi	657,100	2,610,600	25	1986–2016	31
30		Wadi Al Jannah	650,700	2,586,200	220	1987–2015	29
31		Wadi Al Khawd	614,400	2,608,000	71	1986–2013	28
32	Adh Dhahirah	Dakarah	496,725	2,597,564	916	1998–2017	20
33		Dank	424,900	2,606,400	348	1977–2017	41
34		Dhahir	460,765	2,621,761	860	1996–2017	22
35		Kubarah	481,227	2,553,396	481	1995–2017	23
36		Majzi	468,957	2,603,338	738	1997–2016	20
37		Qarn Al Kabsa	469,440	2,585,836	503	1992–2016	25
38		Tanam	445,600	2,559,100	318	1986–2016	31
39	Ad Dakhliyah	Al Qusaiba	508,800	2,494,000	373	1995–2016	22
40		Jiwar	508,100	2,517,500	549	1995–2016	22
41		MOD	572,100	2,543,200	1475	1993–2016	24
42		Musbit	625,400	2,577,600	384	1995–2016	22
43		Najd Al Musallah	503,000	2,541,900	642	1994–2016	23
44		Subayb	515,100	2,567,400	1345	1994–2016	23
45		Tawi Zahir	588,800	2,546,800	748	1994–2016	23
46	Ash Sharqiya North	Ad Dariz	671,300	2,497,700	348	1995–2014	20
47		Al Mudaybi	615,500	2,497,100	409	1994–2014	21
48		Al Muqayhfah	625,600	2,545,400	681	1995–2014	20
49		Haimah	646,000	2,526,300	552	1994–2016	23
50		Ibra	656,300	2,514,500	455	1982–2016	35
51		Masroon	645,300	2,493,900	441	1995–2014	20
52		Wadi Bani Khalid	713,600	2,500,900	624	1995–2016	22
53	Ash Sharqiya South	Al Fujayj	742,900	2,481,900	113	1987–2015	29
54		Fins	725,100	2,538,100	25	1993–2015	23
55		Jaalan Bani	736,700	2,443,900	118	1993–2016	24
56		Jabal Bani Jabir	707,600	2,523,600	1616	1993–2017	25
57		Snaf	738,791	2,500,297	417	1997–2016	20
58		Tahwah	731,100	2,479,100	223	1986–2016	31
59	Dhofar	Aqarhanawt	248,075	1,893,740	937	1996–2016	21
60		Ghadow	179,100	1,895,700	763	1995–2017	23
61		Hagayf	184,600	1,907,200	896	1990–2017	28
62		Mughsayl	164,600	1,871,000	75	1993–2017	25
63		Sadh	294,100	1,887,500	40	1997–2016	20
64		Sher	199,600	1,900,700	525	1997–2017	21
65		Zayk	196,900	1,911,800	831	1987–2016	30

ranging from data investigation of rainfall, flood, earthquake, pollution, environmental quality data, sea currents and other owing to its suitability for modeling maxima (Kotz and Nadarajah, 2000). For the development of IDF curves; it is widely used because of its simplicity (Elsebaie, 2012). In addition, it can be used to reach a higher level of safety by finding higher intensities for shorter duration in the absence of data (Ahmed et al., 2012).

As per Gumbel method the rainfall of specific return period for any desired duration is calculated. The frequency of the precipitation (P_T) in mm for all time intervals with a particular return period (T) in years is computed using the following equations:

$$P_T = P_{avg} + KS \quad (1)$$

Where, K is the Gumbel frequency factor calculated by Eq.(2) as suggested by Chow (1953):

$$K = -\frac{\sqrt{6}}{\pi}\left[0.577 + ln\left[ln\left[\frac{T}{T-1}\right]\right]\right] \quad (2)$$

P_{avg} and S are the average and standard deviation of the maximum precipitation corresponding to a specific duration, calculated using Eq.(3), and Eq.(4), respectively. Where, P_i is the individual extreme value of rainfall, and n is the number of events or years of record.

$$P_{avg} = \frac{1}{n}\sum_{i=n}^{n} P_i \quad (3)$$

$$S = \left[\frac{1}{n-1}\sum_{i=n}^{n}(P_i - P_{avg})^2\right]^{\frac{1}{2}} \quad (4)$$

The K is the function of sample size and the return period, thus when multiplied by standard deviation provides the average rainfall of a desired return period. The rainfall intensity I_T (mm/hr) for the return period T_d is calculated using Eq.(5):

$$I_T = \frac{P_T}{T_d} \quad (5)$$

3.2. Log Pearson III distribution

Log Pearson III distribution is a widely used model to compute the rainfall intensity at different rainfall durations and return period using logarithmically transformation of data (Elsebaie, 2012). Following expressions are used in computation of rainfall intensity:

$$P^* = log(P_i) \quad (6)$$

$$P_T^* = P_{avg}^* + K_T S^* \quad (7)$$

$$P_{avg}^* = \frac{1}{n}\sum_{i-1}^{n} P^* \quad (8)$$

$$S^* = \left[\frac{1}{n-1}\sum_{i=1}^{n}\left(P^* - P_{avg}^*\right)^2\right]^{\frac{1}{2}} \quad (9)$$

$$C_s = \frac{n\sum_i^{ni}\left(P_i^* - P_{avg}^*\right)^3}{(n-1)(n-2)(S^*)^3} \quad (10)$$

Where P_T^*, P_{avg}^* and S^* are as described earlier in Section 3.1; but is established on the logarithmically transformed Pi values as shown in Eq. (6). K_T is known as the Person frequency factor based on Skewness coefficient (C_s) and return period (T). Cs is obtained using Eq. (10); while K_T is obtained using the tables from hydrological references such as Chow et al. (1988). By knowing the recurrence interval and skewness coefficient, the K_T for the distribution is obtained. Further, the antilog of the solution in Eq. (7) determines the estimated extreme value for the given return period.

3.3. Derivation of IDF empirical formula

The relationship between the rainfall intensity (I), rainfall duration (d), and the return period (T_R) is defined by the IDF empirical formula. Several steps are followed to establish an equation for the calculation of rainfall intensity for a specific rainfall period and recurrence interval, which is dependent mainly on the results from the IDF curves. In the study the widely used Bernard equation (Bernard, 1932) is selected to establish the IDF relationship. The following steps and equations were used to the IDF relationship:

$$I = \frac{C{T_R}^m}{d^e} \quad (11)$$

Where, I is the rainfall intensity (mm/hr), d is the rainfall duration (minutes), T is the return period (years) and the empirical parameters (C, m, and e). Using logarithmic transformation Eq. (11) can be expressed as:

$$\log I = \log(C{T_R}^m) - e\log d \quad (12)$$

Further, for a particular T, considering K as a constant:

$$K = C{T_R}^m \quad (13)$$

Eq. (7) is rewritten as:

$$\log I = \log K - e\log d \quad (14)$$

The plot of the logarithm of rainfall intensity (log I) against the logarithm of time (log d) for a specific return period results in a straight line for Eq.(13). From the linear relation the value of log K (intercept) and e (slope) are derived from each return period plot. The average of the values of e represents the empirical parameter e. The parameter C and m is obtained using logarithmic transformation of Eq. (13):

$$\log K = \log C + m\log T_R \quad (15)$$

By plotting the log K and log T_R in the straight line, the slope (m) and intercepts (log C) are derived. Finally, the values of C, m, and e are substituted in Eq. (11) to obtain the IDF equation.

3.4. Goodness of fit test

The least squares goodness of fit method was also used to evaluate the difference between the observed and calculated rainfall intensities of selected distribution. The goodness of fit is checked using the calculation of coefficient of determination (R^2) using Eq. (17).

$$R^2 = 1 - \frac{\sum_{i=1}^{n}(X_i - Y_i)^2}{\sum_{i=1}^{n}\left(\bar{Y} - Y_i\right)^2} \quad (17)$$

Where, Xi and Yi are observed and estimated data at time i, $\bar{Y}$ is mean of estimated data and n is total number of data points.

3.5. Contour plots

The contours of the calculated IDF parameters were plotted using SURFER software. The software is mostly used for 3D surface mapping, contour mapping, terrain modeling and others. Kriging interpolation method was used for contouring of the parameters. It is a best unbiased linear estimation method (Isaaks and Srivastava, 1989); and a flexible gridding method that incorporates underlying trends and anisotropy in the natural and efficient manner (Yang et al., 2004).

4. Result and discussion

4.1. Rainfall analysis

Statistical analysis of the annual rainfall (total rainfall) for 65 study location of Oman from year 1977 to 2017 is shown in Table 2. All the monitoring stations have demonstrated highly variable annual rainfall over the study period. Both annual maximum rainfall of 806.29 mm (Wadi Al Koudh in year 2004) and minimum rainfall of 9.39 mm (Ruwi in year 2003) were observed in Muscat governorate. The Skewness coefficient and Kurtosis coefficient measures the asymmetry and peakedness or flatness of the frequency distribution of the data (Sheskin, 2000). Negative kurtosis and positive kurtosis values indicate the distribution is flatter and sharper in its center than the normal distribution, respectively. Kurtosis coefficient is in the range of −1.429 to 8.167 during the study period that shows higher occurrence of probability near the mean than that in the normal distribution. Skewness coefficient in the range of 0.1 to 2.66 was observed for the stations. The observed positive skewed distribution exhibits much less frequency of occurrence of higher intensity rainfalls and the high frequency of occurrence of annual rainfall below the mean value (see Table 2).

The average annual rainfall exhibited for all studied stations from 1977 to 2017 is 109.21 mm with a standard deviation of 92.82 mm, Skewness coefficient of 1.62 and Kurtosis coefficient of 3.08. The observed highest average annual rainfall is 307.1 mm at Subayb, followed by 190.45 mm at Jabal Bani Jabir, 185.22 mm at Rhaibah and, 180.21 at MOD. While the lowest average of 38.41 mm at Al Qusaiba, succeeded by 48.30 mm at Khatwah, 61.15 mm at Tanam, and 61.64 mm at Kubarah. Interestingly, both highest and lowest average annual rainfall was recorded in Ad-Dakhliyah goveronate. Geographically, Subayb, is in the mountainous range at 1345 m elevation, while Al-Qusaiba station is situated in the flat terrain closer to the Al-Wusta desert region at 373 m elevation. Thus, the study shows that the rainfall in the mountainous region is high compared to the desert and the coastal region of the country. Fig. 2 presents the box and whisker plot of annual rainfall at studied governorates during monitoring period. The dataset exhibits the upward or positive skewness in all governorate with average rainfall higher than the median rainfall.

Variation of average annual rainfall (total rainfall) in various governorates of Oman from 1986 to 2016 is shown in Fig. 3. The highest average of 432.74 mm was recorded in 1997 in Musandam governorate located at the Northern Oman. The years 1990 (382.22 Ash-Sharqiya North), 1997 (360.21 at Ad-Dakhliyah), 2007 (361.21 mm at Muscat), and 2010 (347.37 at Ash-Sharqiya South) also recorded the high average rainfall. The lowest average of 20.64 mm was observed in the year 2008 in Ash-Sharqiya North. Similarly, lowest averages were recorded in the years 2001 (20.68 mm at Al-Buraimi), 2008 (21.09 at Ash-Sharqiya North), 2001 (21.28 at Adh-Dhahirah), and 1985 (23.30 mm Muscat). For the study period of 1986 to 2016, a slightly negative trend in average annual rainfall of −1.195 mm/years was observed for overall stations (Fig. 3). Among the studied region, Musandam governorate in northern part of Oman has the highest annual average of 149.81 mm followed by Mountainous area Ad-Dakhaliyah (130.06 mm). The annual average of 113.54 mm, 111.54 mm, 108.02 mm, and 102.54 mm were observed in Dhofar, Al-Batinah South, Ash-Sharqia North and Muscat governorates. While the lowest annual averages were observed at Ash-Sharqiyah North (95.56 mm), Al-Batinah North (91.84 mm), Adh-Dhahirah (83.04 mm) and Al-Buraimi (82.838 mm).

4.2. Intensity-Duration-Frequency (IDF) relationships

Gumbel and Log Pearson Type III distribution were mostly used distribution in arid region in IDF calculation. So, initially both distributions were used at Wadi Al Jannah station to check the best distribution using maximum rainfall records. Rainfall intensities for all the stations is estimated for corresponding rainfall duration (5, 15, 30, 60, 360, 720 and 1440 min) and return periods (2, 5, 10, 25, 50, and 100). Fig. 4 shows the observed and modeled intensity of two distribution; while Table 3 presents the summary of best fit result between two distribution using coefficients of determination (R^2) using Eq. (17) at various return periods. Both models showed the good correlation with values greater than 0.9 at all return period. As best fit result did not showed any major difference two distribution, Gumbel distribution is further used in all the stations in this study.

Table 4 and Fig. 5 shows the calculated rainfall intensities at Rhibah, Aqbat Al-Risah, Wadi Al-Jannah, Subayb, and Mughsayl stations for return periods of 2, 5, 10, 25 and 100 years using Gumbel distribution. The estimation showed the rainfall intensities increased with the return period, while the intensities decreased with the increase in the rainfall duration at all the stations. Subayb station at Ad-Dakhliah, the site with higher annual rainfall is likely to experience high rainfall with longer duration and return period compared to other stations.

Also, higher intensity rainfall at various return periods were witnessed at the higher elevation stations compared to the lower elevation stations. Among the stations presented in Table 4 and Fig. 5, Subayb (elevation 1345 m) has the highest rainfall while Mughsayl (elevation 25 m) has the lowest rainfall for all the return periods as compared to the other stations. Similar observations were reported by Kotoub (2004), where the rational method was used to evaluate the rainfall intensities at various return period for Plain, Hills and Mountains region of Oman, for flood peak and wadi characteristic studies for road network development. These studies showed among three studied regions of Oman, Mountains have the higher intensities rainfall followed by Hills, and Plains has the lowest intensities rainfall for various return periods. Thus, in the mountainous region the estimated rainfall intensities for various return periods are high as compared to the desert or interior region, and the coastal region of the country (Table 4; Fig. 5).

4.3. Intensity-Duration-Frequency (IDF) equation

Estimation of the empirical parameters (C, m, and e) of IDF relationship (Eq. (6) was done using nonlinear regression analysis in Microsoft Excel. Goodness of fit between observed and estimated data was checked using R^2 values. IDF curve for Khasab, Wadi Salmah, Saham, Dhabaah, Wadi Al-Jannah, Dank, Subayb, Ibra, Tahwa and Mughsayl stations presented in log scale are shown in Fig. 4. Also, the IDF curves are parallel to each other (Fig. 6). Table 5 shows the estimated IDF parameter values, IDF equation with R^2 achieved by IDF data analysis. The empirical parameter values for C ranged from 417.5 to 8.95, m ranged from 0.645 to 0.196, and e ranged from 0.79 to 0.391 for the studied stations. The obtained results showed good correlation between the observed and estimated rainfall intensities with high R^2 ranging between 0.994 and 0.851 (Table 5). Therefore, the IDF curved generated at the stations could be further used in the rainfall estimation and in design of water related projects in Oman.

4.4. Empirical IDF parameter contours

The spatial distribution maps of the IDF parameters C, m, and e are shown in Fig. 7. The contours show the smooth variation of parameter over the whole country. But, Due to the absence of monitoring points in the Al-Wusta region, contour lines generated in the middle section of the country are based on the interpolation of data from the neighboring regions. Also, the data from adjacent countries Saudi Arabia and United Arab Emirates were included. Thus, the contour lines extending beyond the Oman's border were based on the interpolation only.

All parameter values are relatively high and more condensed in the Northern part of the country compared to the Southern part.

Table 2
Statistical information of annual rainfall (mm) at the monitoring stations.

Governorate	Station Name	Maximum (mm)	Minimum (mm)	Average (mm)	Standard Deviation (mm)	Skewness Coefficient	Kurtosis Coefficient
Musandam	Ghamda	536.15	15.79	165.11	125.24	1.14	0.99
	Khasab	426.43	10.11	136.54	109.98	1.07	0.60
	Rhaibah	515.36	17.73	185.22	126.61	0.75	0.15
	Sal Ala	489.34	17.64	123.25	110.69	1.80	3.42
	Sima	438.03	13.20	128.53	99.02	1.38	1.99
Al-Buraimi	Al-Juwayf	344.87	23.23	99.97	80.19	1.88	3.87
	Al-Ubaylah	302.11	10.04	69.81	72.73	2.01	4.51
	Fayyad	270.44	15.21	96.84	63.02	1.20	1.51
	Khatwah	274.45	17.33	48.30	66.00	2.66	7.19
	Mahdah	285.10	18.80	95.37	70.89	0.88	0.34
	Wadi Salmah	224.97	19.43	64.63	48.30	1.47	2.79
	Wadi Sharm	269.08	10.07	80.40	63.86	1.17	1.45
Al Batinah North	Al-Ghuzayfah	326.91	9.66	88.61	74.73	1.99	3.91
	Al-Jizzi	203.23	16.35	74.05	51.45	1.09	0.44
	Aqair Al-Abreein	415.50	13.53	110.78	108.96	1.61	2.35
	Aqbat Al-Risah	319.66	14.16	92.97	84.92	1.45	1.45
	Hayl Al-Najd	486.00	20.03	102.72	106.91	2.63	6.62
	Saham	275.56	11.35	78.74	64.28	1.31	1.88
Al-Batinah South	Al-Miseen	460.37	13.63	127.50	100.06	1.74	4.46
	Al-Wasit	252.78	15.93	76.01	69.18	1.38	0.64
	Ar-Rustaq	297.25	12.36	103.06	79.76	0.94	0.16
	Barka	178.98	13.22	66.79	37.00	1.29	2.23
	Dhabaah	558.76	19.58	155.03	111.35	1.58	3.98
	Salma	374.25	11.73	161.92	111.20	0.23	−1.09
Muscat	Buei	469.21	18.44	124.22	125.00	1.53	1.83
	Hayfadh	672.08	15.02	83.36	150.11	2.37	6.12
	Mazara 3	526.25	13.65	136.92	121.18	1.77	3.22
	Muscat	271.03	10.95	70.67	68.34	1.93	3.16
	Ruwi	346.40	9.39	111.26	79.25	0.96	1.14
	Wadi Al-Jannah	166.60	39.83	62.81	25.60	2.61	7.07
	Wadi Al-Khawd	860.29	17.83	120.66	213.61	2.52	8.17
Adh-Dhahirah	Dakarah	410.22	14.60	108.80	96.80	1.93	4.25
	Dank	331.43	10.81	69.40	74.16	2.18	5.34
	Dhahir	368.31	10.04	92.39	90.38	1.74	3.60
	Kubarah	200.82	16.27	61.64	50.09	1.40	2.23
	Majzi	536.76	18.19	105.32	130.82	2.30	5.88
	Qarn Al-Kabsa	282.05	19.28	74.03	71.26	1.65	2.66
	Tanam 2	196.20	13.56	61.14	50.34	1.14	0.59
Ad-Dakhliyah	Al-Qusaiba	169.64	12.11	38.41	42.72	1.99	4.10
	Jiwar	249.47	18.07	64.37	62.74	1.43	2.39
	MOD	734.87	23.96	180.21	155.67	2.15	6.31
	Musbit	279.87	11.68	78.73	66.20	1.93	3.99
	Najd Al-Musallah	331.48	10.20	104.79	81.14	1.14	1.39
	Subayb	655.50	27.50	307.10	225.47	0.16	−1.43
	Tawi Zahir	497.43	11.99	142.37	109.00	1.85	4.79
Ash-Sharqiya North	Ad-Dariz	334.47	17.08	72.57	81.71	1.97	4.80
	Al-Mudaybi	331.62	12.66	73.02	79.98	2.05	4.66
	Al-Muqayhfah	334.47	16.08	73.07	81.55	1.96	4.81
	Haimah	392.14	11.25	127.87	110.70	1.47	1.28
	Ibra	382.48	10.49	113.17	96.76	1.47	1.49
	Masroon	344.81	12.57	80.05	76.89	2.46	7.21
	Wadi Bani Khalid	514.33	13.24	129.17	126.03	1.82	3.41
Ash-Sharqiya South	Al-Fuljayj	442.46	10.65	84.90	95.27	2.39	6.80
	Fins	306.30	14.86	93.68	78.06	1.22	1.02
	Jaalan Bani	216.87	20.09	64.64	49.94	2.51	5.93
	Jabal Bani Jabir	765.23	36.53	190.45	165.53	1.97	5.07
	Snaf	368.80	20.70	107.10	106.68	1.31	0.75
	Tahwah 3	442.46	12.36	84.69	91.69	2.52	7.57
Dhofar	Aqarhanawt	438.00	19.01	141.98	125.26	1.30	0.83
	Ghadow	676.93	22.05	136.92	159.37	2.01	5.03
	Hagayf	411.15	11.95	108.61	102.48	2.03	3.98
	Mughsayl	173.97	13.52	83.34	45.09	0.10	−0.78
	Sadh	156.41	33.21	66.45	34.20	1.38	1.35
	Sher	394.35	14.20	154.10	126.92	0.76	−0.56
	Zayk 1	340.50	10.46	98.05	73.22	1.09	2.73
All Stations		**860.29**	**7.83**	**109.21***	**92.82***	**1.62***	**3.08***

Note: * represents the average values.

Particularly, the high values were observed along the Al-Hajar mountain range that runs parallel to the Al Batinah Coast. Values of the parameters are lower at the flat areas than the ones in the higher altitude areas of Al Batinah region. Also, the values were observed declining steadily along the coastal plains. There is no literature found on the generation of IDF curve and its parameters at

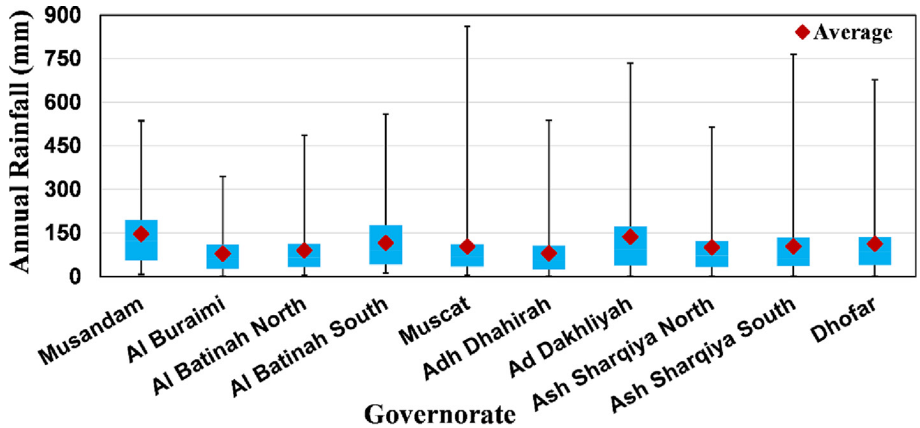

Fig. 2. Box and Whisker plot showing annual rainfall at different governorate during study period.

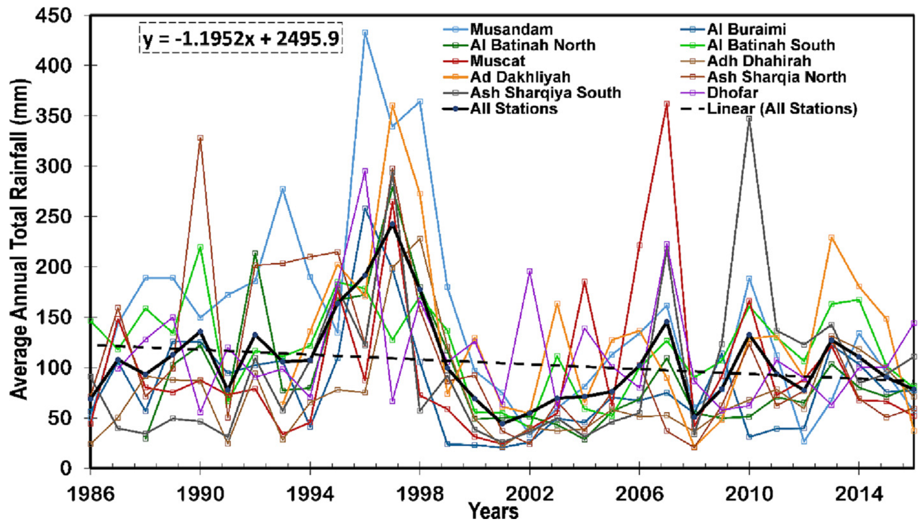

Fig. 3. Variation of average annual total rainfall in various governorate.

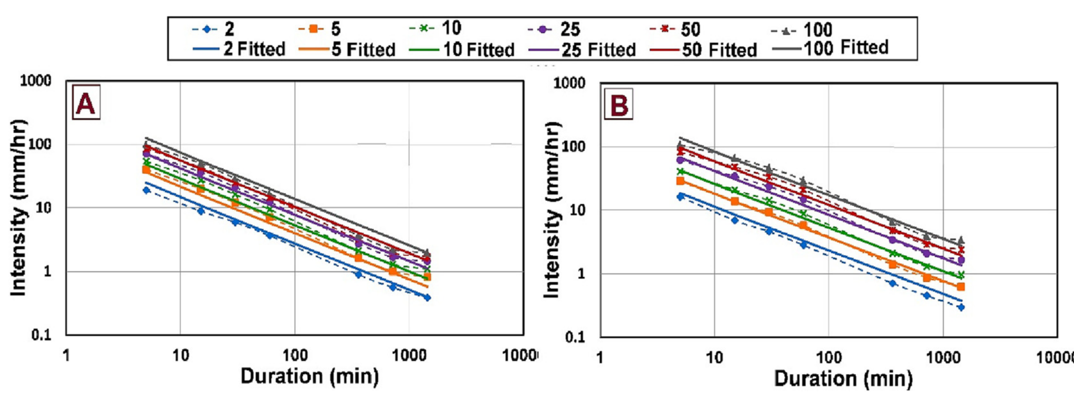

Fig. 4. Observed and Modeled rainfall intensity at Wadi Al Jannah Station using A) Gumbel and B) Log Pearson Type III distributions at various return periods (2, 5, 10, 25, 50, 100 years).

Table 3
Summary of best fit distribution at various return periods for Wadi Al Jannah station.

Distribution	Return Period					
	2	5	10	25	50	100
	Coefficient of Determination (R^2)					
Gumbel	0.998	0.995	0.992	0.992	0.992	0.991
Log-Pearson Type III	0.999	0.997	0.995	0.991	0.988	0.985

Table 4
Rainfall Intensity (mm/hr) at Rhibah, Aqbat Al Risah, Wadi Al Jannah, Subayb and Mughsayl station at various duration and return period using Gumbel Distribution.

Station (Governorate)	Elevation (m)	Rainfall Duration, d (hr)	Return Period, T (Years)					
			2	5	10	25	50	100
			Frequency Factor, K					
			−0.1644	0.7198	1.3052	2.0449	2.5936	3.1383
			Rainfall Intensity-I (mm/hr)					
Rhibah (Musandam)	704	0.833	36.04	69.90	92.32	120.65	141.67	162.53
		0.25	21.65	41.04	53.88	70.11	82.15	94.10
		0.5	16.58	29.19	37.54	48.09	55.91	63.68
		1	11.92	19.54	24.59	30.97	35.71	40.40
		360	3.58	6.16	7.87	10.03	11.63	13.22
		720	2.50	3.97	4.94	6.17	7.08	7.98
		1440	1.71	2.60	3.19	3.93	4.48	5.02
Aqbat Al-Risah (Al-Batinah North)	516	0.833	44.34	74.18	93.93	118.89	137.41	155.78
		0.25	26.36	43.81	55.37	69.98	80.81	91.57
		0.5	17.51	30.73	39.48	50.54	58.74	66.88
		1	11.14	19.69	25.35	32.50	37.80	43.07
		360	2.32	4.05	5.20	6.66	7.74	8.80
		720	1.38	2.27	2.86	3.60	4.16	4.71
		1440	0.87	1.39	1.72	2.15	2.47	2.78
Wadi Al-Jannah (Muscat)	220	0.833	18.78	39.97	54.00	71.72	84.87	97.92
		0.25	8.87	19.80	27.04	36.19	42.97	49.70
		0.5	5.94	12.07	16.13	21.26	25.06	28.84
		1	3.65	7.12	9.42	12.33	14.48	16.62
		360	0.89	1.63	2.12	2.74	3.20	3.65
		720	0.56	1.00	1.30	1.67	1.95	2.22
		1440	0.39	0.81	1.09	1.45	1.71	1.97
Subayb (Ad- Dakhaliyah)	1345	0.833	116.65	167.11	200.52	242.73	274.05	305.13
		0.25	74.58	114.22	140.47	173.63	198.23	222.64
		0.5	51.15	80.74	100.32	125.07	143.43	161.66
		1	30.39	47.92	59.52	74.18	85.05	95.85
		360	8.06	13.32	16.80	21.19	24.46	27.69
		720	4.43	7.60	9.70	12.35	14.32	16.27
		1440	2.60	4.5	5.76	7.35	8.53	9.70
Mughsayl (Dhofar)	25	0.833	15.29	35.23	48.42	65.10	77.47	89.75
		0.25	8.24	18.91	25.97	34.89	41.51	48.08
		0.5	5.69	12.50	17.01	22.71	26.93	31.13
		1	3.94	7.71	10.21	13.36	15.70	18.02
		360	1.10	2.20	2.93	3.86	4.54	5.22
		720	0.76	1.44	1.90	2.47	2.90	3.32
		1440	0.51	0.92	1.19	1.53	1.78	2.03

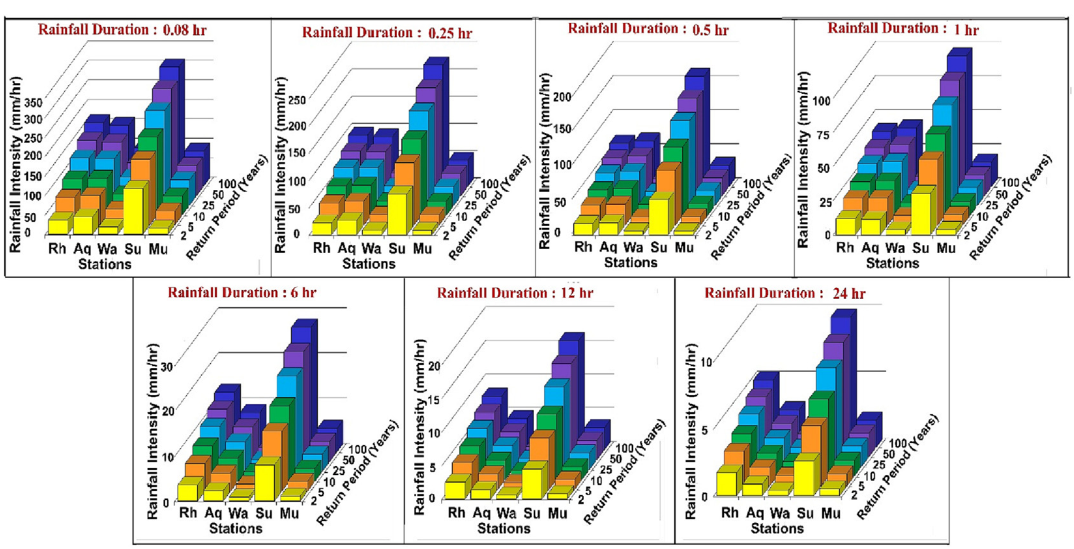

Fig. 5. Rainfall intensity at different durations and return periods at Rh (Rhibah), Aq (Aqbal Al-Risah), Wa (Wadi Al Jannah), Su (Subayb), and Mu (Mughsayl) stations.

the various stations covering whole of Oman. Therefore, the generated contour maps could be used to estimate the empirical parameters; construct the IDF formula and curves and estimate the rainfall intensities for various rainfall duration and return periods at ungauged locations. Especially in the arid region where the rainfall is erratic and unpredictable with both space and time local IDF

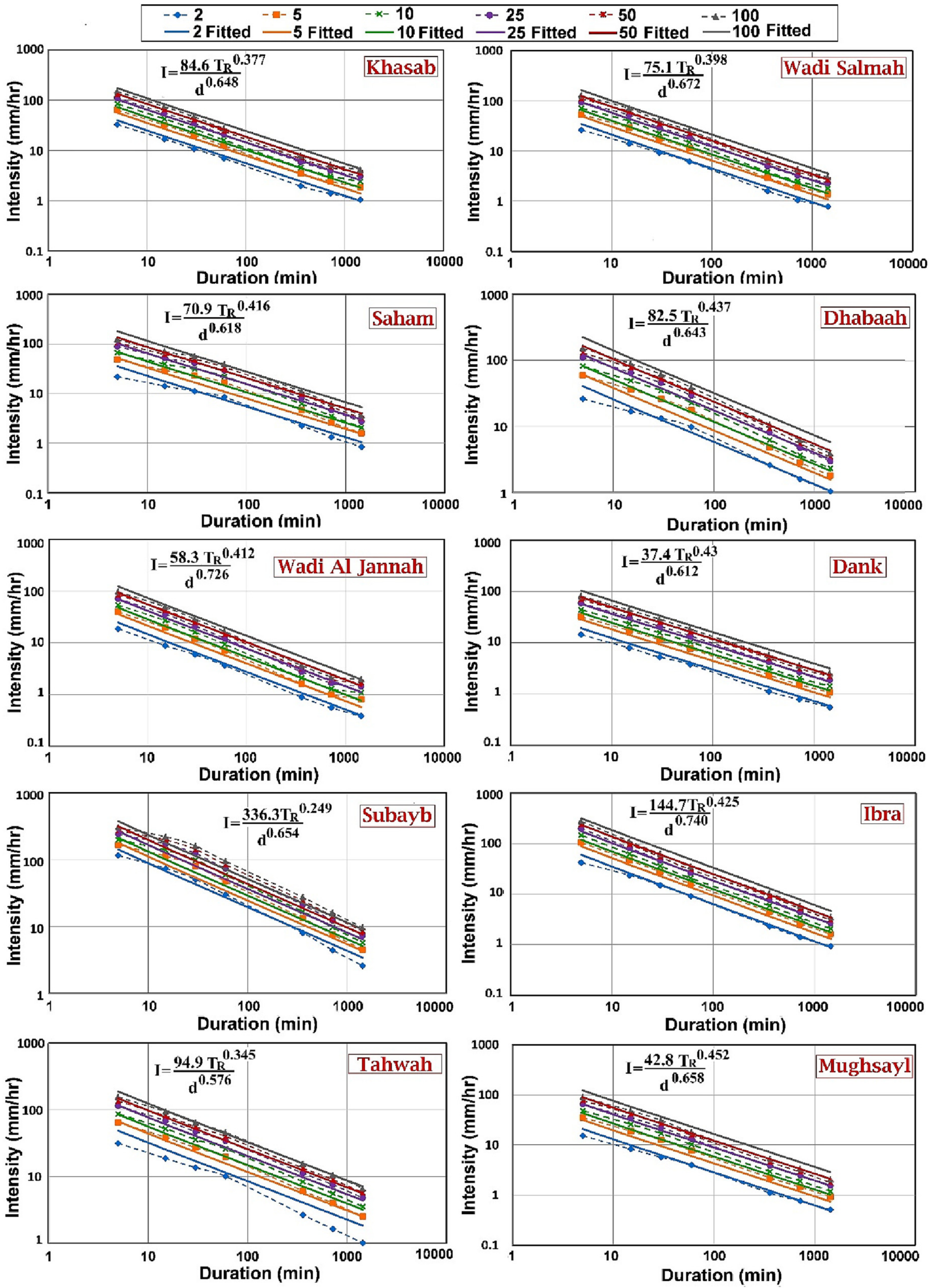

Fig. 6. IDF curve for Khasab, Wadi Salmah, Saham, Dhabaah, Wadi Al-Jannah, Dank, Subayb, Ibra, Tahwa, and Mughsayl station.

Table 5
IDF parameter and equation with coefficient of determination for studied stations.

Governorate	Station Name	IDF Parameters			IDF Formula ($I = \frac{CT_R{}^m}{d^e}$)	Coefficient of determination (R^2)
		C	m	e		
Musandam	Ghamda	73.3	0.435	0.641	$I = \frac{73.3T_R{}^{0.435}}{d^{0.641}}$	0.914
	Khasab	84.6	0.377	0.648	$I = \frac{84.6T_R{}^{0.377}}{d^{0.648}}$	0.931
	Rhaibah	71.4	0.405	0.599	$I = \frac{71.4T_R{}^{0.405}}{d^{0.599}}$	0.930
	Sal Ala	24.0	0.645	0.596	$I = \frac{24T_R{}^{0.645}}{d^{0.596}}$	0.861
	Sima	33.6	0.580	0.614	$I = \frac{33.6T_R{}^{0.58}}{d^{0.614}}$	0.870
Al-Buraimi	Al-Juwayf	144.6	0.319	0.713	$I = \frac{144.6T_R{}^{0.319}}{d^{0.713}}$	0.994
	Al-Ubaylah	111.5	0.317	0.713	$I = \frac{111.5T_R{}^{0.317}}{d^{0.713}}$	0.948
	Fayyad	168.0	0.279	0.685	$I = \frac{168T_R{}^{0.279}}{d^{0.685}}$	0.990
	Khatwah	27.8	0.390	0.575	$I = \frac{27.9T_R{}^{0.39}}{d^{0.575}}$	0.926
	Mahdah	65.4	0.403	0.627	$I = \frac{65.4T_R{}^{0.403}}{d^{0.627}}$	0.934
	Wadi Salmah	75.1	0.398	0.672	$I = \frac{75.1T_R{}^{0.398}}{d^{0.672}}$	0.924
	Wadi Sharm	145.5	0.371	0.691	$I = \frac{145.5T_R{}^{0.371}}{d^{0.691}}$	0.932
Al-Batinah North	Al-Ghuzayfah	9.0	0.347	0.413	$I = \frac{9T_R{}^{0.347}}{d^{0.413}}$	0.937
	Al-Jizzi	130.6	0.444	0.746	$I = \frac{130.6T_R{}^{0.444}}{d^{0.746}}$	0.915
	Aqair Al-Abreein	70.9	0.416	0.618	$I = \frac{70.9T_R{}^{0.416}}{d^{0.618}}$	0.918
	Aqbat Al-Risah	166.1	0.325	0.734	$I = \frac{166.1T_R{}^{0.325}}{d^{0.734}}$	0.946
	Hayl Al-Najd	229.8	0.313	0.740	$I = \frac{229.8T_R{}^{0.313}}{d^{0.74}}$	0.851
	Saham	70.9	0.416	0.618	$I = \frac{70.9T_R{}^{0.416}}{d^{0.618}}$	0.918
Al-Batinah South	Al-Miseen	168.9	0.301	0.651	$I = \frac{168.9T_R{}^{0.301}}{d^{0.651}}$	0.953
	Al-Wasit	137.6	0.350	0.683	$I = \frac{137.6T_R{}^{0.35}}{d^{0.683}}$	0.939
	Ar-Rustaq	129.5	0.360	0.664	$I = \frac{129.5T_R{}^{0.36}}{d^{0.664}}$	0.936
	Barka	90.1	0.566	0.742	$I = \frac{90.1T_R{}^{0.566}}{d^{0.742}}$	0.963
	Dhabaah	82.5	0.437	0.643	$I = \frac{82.5T_R{}^{0.437}}{d^{0.643}}$	0.913
	Salma	176.4	0.311	0.652	$I = \frac{176.4T_R{}^{0.311}}{d^{0.652}}$	0.949
Muscat	Buei	157.8	0.324	0.577	$I = \frac{157.8T_R{}^{0.324}}{d^{0.577}}$	0.957
	Hayfadh	74.8	0.216	0.391	$I = \frac{74.8T_R{}^{0.216}}{d^{0.391}}$	0.991
	Mazara	99.0	0.303	0.743	$I = \frac{99T_R{}^{0.303}}{d^{0.743}}$	0.960
	Muscat	42.8	0.452	0.658	$I = \frac{42.8T_R{}^{0.452}}{d^{0.658}}$	0.922
	Ruwi	167.0	0.307	0.644	$I = \frac{167T_R{}^{0.307}}{d^{0.644}}$	0.990
	Wadi Al-Jannah	58.3	0.412	0.726	$I = \frac{58.3T_R{}^{0.412}}{d^{0.726}}$	0.920
	Wadi Al-Khawd	109.2	0.453	0.568	$I = \frac{109.2T_R{}^{0.453}}{d^{0.568}}$	0.949
Adh-Dhahirah	Dakarah	205.1	0.211	0.654	$I = \frac{205.1T_R{}^{0.211}}{d^{0.654}}$	0.977
	Dank	37.4	0.430	0.612	$I = \frac{37.4T_R{}^{0.43}}{d^{0.612}}$	0.914
	Dhahir	170.9	0.266	0.703	$I = \frac{170.9T_R{}^{0.266}}{d^{0.703}}$	0.961
	Kubarah	175.2	0.373	0.775	$I = \frac{175.2T_R{}^{0.373}}{d^{0.775}}$	0.932
	Majzi	193.8	0.304	0.733	$I = \frac{193.8T_R{}^{0.304}}{d^{0.733}}$	0.951
	Qarn Al-Kabsa	97.6	0.458	0.694	$I = \frac{97.6T_R{}^{0.458}}{d^{0.694}}$	0.914
	Tanam	89.7	0.384	0.683	$I = \frac{89.7T_R{}^{0.384}}{d^{0.683}}$	0.939
Ad-Dakhliyah	Al Qusaiba	177.0	0.299	0.708	$I = \frac{177T_R{}^{0.299}}{d^{0.708}}$	0.959
	Jiwar	175.6	0.398	0.790	$I = \frac{175.6T_R{}^{0.398}}{d^{0.790}}$	0.924
	MOD	309.4	0.196	0.681	$I = \frac{309.4T_R{}^{0.196}}{d^{0.681}}$	0.980
	Musbit	381.0	0.248	0.653	$I = \frac{381T_R{}^{0.248}}{d^{0.653}}$	0.973
	Najd Al-Musallah	251.6	0.332	0.753	$I = \frac{251.6T_R{}^{0.332}}{d^{0.753}}$	0.990
	Subayb	417.5	0.249	0.654	$I = \frac{336.3T_R{}^{0.249}}{d^{0.654}}$	0.972
	Tawi Zahir	263.3	0.219	0.685	$I = \frac{26.3T_R{}^{0.219}}{d^{0.685}}$	0.994

(*continued on next page*)

Table 5 (*continued*)

Governorate	Station Name	IDF Parameters			IDF Formula ($I = \frac{CT_R^m}{d^e}$)	Coefficient of determination (R^2)
		C	m	e		
Ash Sharqiya North	Ad-Dariz	180.1	0.211	0.606	$I = \frac{180.1T_R^{0.211}}{d^{0.606}}$	0.956
	Al-Mudaybi	195.1	0.218	0.676	$I = \frac{195.1T_R^{0.218}}{d^{0.676}}$	0.994
	Al-Muqayhfah	179.8	0.294	0.696	$I = \frac{179.8T_R^{0.294}}{d^{0.696}}$	0.956
	Haimah	265.8	0.237	0.685	$I = \frac{265.8T_R^{0.237}}{d^{0.685}}$	0.969
	Ibra	144.7	0.425	0.740	$I = \frac{144.7T_R^{0.425}}{d^{0.74}}$	0.914
	Masroon	114.1	0.407	0.741	$I = \frac{114.1T_R^{0.407}}{d^{0.741}}$	0.955
	Wadi Bani Khalid	279.0	0.238	0.670	$I = \frac{279T_R^{0.238}}{d^{0.67}}$	0.973
Ash-Sharqiya South	Al-Fujayj	102.1	0.352	0.583	$I = \frac{102.1T_R^{0.352}}{d^{0.583}}$	0.940
	Fins	168.1	0.245	0.631	$I = \frac{168.1T_R^{0.245}}{d^{0.631}}$	0.969
	Jaalan Bani	45.9	0.242	0.569	$I = \frac{45.9T_R^{0.242}}{d^{0.569}}$	0.970
	Jabal Bani Jabir	105.1	0.397	0.580	$I = \frac{105.1T_R^{0.397}}{d^{0.580}}$	0.924
	Snaf	148.6	0.214	0.547	$I = \frac{148.6T_R^{0.214}}{d^{0.547}}$	0.985
	Tahwah	94.9	0.345	0.576	$I = \frac{94.9T_R^{0.345}}{d^{0.576}}$	0.943
Dhofar	Aqarhanawt	37.6	0.584	0.552	$I = \frac{37.6T_R^{0.584}}{d^{0.552}}$	0.968
	Ghadow	25.8	0.632	0.566	$I = \frac{25.8T_R^{0.632}}{d^{0.566}}$	0.929
	Hagayf	71.4	0.405	0.548	$I = \frac{71.4T_R^{0.405}}{d^{0.548}}$	0.912
	Mughsayl	42.8	0.452	0.658	$I = \frac{42.8T_R^{0.452}}{d^{0.658}}$	0.908
	Sadh	90.4	0.268	0.651	$I = \frac{90.4T_R^{0.268}}{d^{0.651}}$	0.968
	Sher	114.1	0.407	0.645	$I = \frac{114.1T_R^{0.407}}{d^{0.645}}$	0.921
	Zayk	52.4	0.507	0.635	$I = \frac{52.4T_R^{0.507}}{d^{0.635}}$	0.887

curves development would be valuable. Also, using new IDF curve concentrated in the actual study area rather than using one generalized regional IDF curve will provide appropriate rainfall data for flood, storm water, road-bridge design and other environmental studies.

5. Conclusions

Intensity–duration–frequency (IDF) curves are utilized in the hydrologic and water engineering projects water resource projects in planning and designing of storm drainage, flood protection, bridges and culverts, water impounding facilities, and other water resources systems. In this study the development of IDF curves was done using Bernard's equation. Gumbel distribution was used to obtain rainfall intensities for various durations and return periods. The historical rainfall data obtained from the Ministry of Regional Municipalities and Water Resources (MRMWR) at 65 gauging stations situated at different elevation and regions throughout Oman were used in the study. IDF curves and empirical formulas were derived for rainfall durations (5, 15, 30, 60, 360, 720, and 1440 min) for various return periods (2, 5, 10, 25, 50, and 100 years).

Rainfall analysis exhibited the average annual rainfall of 109.21 mm with a standard deviation of 92.82 mm, Skewness coefficient of 1.62 and Kurtosis coefficient of 3.08 for all the studied stations from 1977 to 2017. The study also shows that the rainfall in the mountainous region is high compared to the desert and the coastal region of the country. Also, IDF analysis indicated the higher intensity rainfall at various return periods was witnessed at the higher elevation stations compared to the lower elevation stations. IDF empirical parameters estimation using nonlinear regression provided the parameter values for *C* ranging from 417.5 to 8.95, *m* ranging from 0.645 to 0.196, and *e* ranging from 0.79 to 0.391 for the studied stations.

Finally, the contour maps of spatial distribution of the IDF parameters were plotted for whole country. The parameter values were moderately high and more condensed in the northern part of the country along the Al-Hajar mountain range as compared to the southern part and along the flat terrain of the country. The created contour maps may be helpful in estimating the empirical parameters of the IDF formula and then estimate the rainfall intensities for various rainfall durations and return periods at ungauged locations. The outcome of this study will be helpful in planning, designing and decision making of future water resources and urban drainage projects.

In addition to sampling error, errors due to weather and climate change, and model errors from the short length of data also cause uncertainties in design of rainfall estimation. In any hydraulic and hydrologic structure, the design flow is usually considered for 100 years. Therefore, in this study the rainfall intensities for 100 years were considered despite the short length of rainfall data. So it is recommended to use sufficient length of rainfall data and to use uncertainty analysis methods (Bayesian methods, Cross validation approaches, Bootstrapping, and other methods) in designs to increase credibility of any project. The preliminary research in development of IDF curves in Oman is presented in this study. However, development of regional and more comprehensive studies along with detailed orographic factors in in addition to elevation are intended, in collaboration with neighboring GCC and other countries.

Declaration of Competing Interest

The authors declare that they have no known competing financial interests or personal relationships that could have appeared to influence the work reported in this paper.

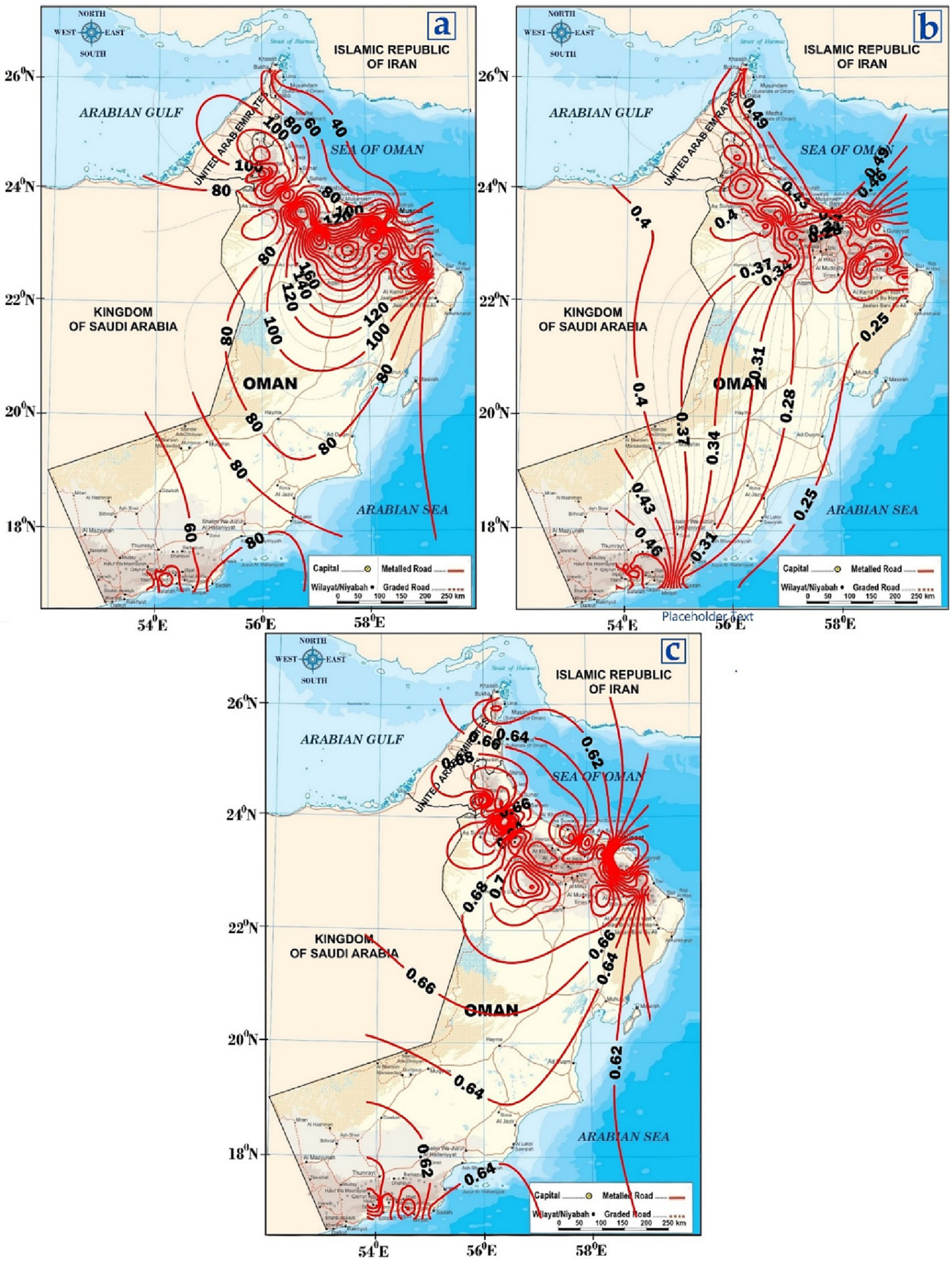

Fig. 7. Spatial distribution contour map of empirical IDF parameters (a) *C*, (b) *m*, and (c) *e*.

Acknowledgement

The authors would like to thank the Ministry of Agriculture, Fisheries Wealth and Water Resources, Sultanate of Oman for providing the data used in the present study.

References

Ahmed, Z., Rao, D., Reddy, K., Raj, E., 2012. Rainfall intensity variation for observed data and derived data - a case study of Imphal. ARPN Journal of Engineering and Applied Sciences 11 (7), 1506–1513.

Al Areeq, A., Al Zahrani, M., Chowdhury, S., 2021. Rainfall Intensity–Duration–Frequency (IDF) Curves: Effects of Uncertainty on Flood Protection and Runoff Quantification in Southwestern Saudi Arabia. Arab. J. Sci. Eng. 46, 10993–11007. https://doi.org/10.1007/s13369-021-06142-0.

Al Barwani, A. 2014. Water Resources Management Practices in the Sultanate Oman. Paper presented at the The Third International Conference on Water Resources and Environmental Management (GIWEH), Antalya, Turkey.

Al Shaikh, A.A., 1985. Rainfall frequency studies for Saudi Arabia. King Saud University, Riyadh. M.Sc. Thesis M.Sc. Thesis,.

Al-Amri, N.S., Subyan, A.M., 2017. Generation of Rainfall Intensity Duration Frequency (IDF) Curves for Ungauged Sites in Arid Region. Earth Syst. Environ. 1 (8). https://doi.org/10.1007/s41748-017-0008-8.

Al-anazi, K.K., El-Sebaie, I.H., 2013. Development of Intensity-Duration-Frequency Relationships for Abha City in Saudi Arabia. International Journal of Computational Engineering Research 3 (10), 58–65.

Aldosari, D., Almedeij, J., Alsumaiei, A.A., 2020. Update of intensity–duration–frequency curves for Kuwait due to extreme flash floods. Environ. Ecol. Stat. 27, 491–507. https://doi.org/10.1007/s10651-020-00454-4.
AlHassoun, S.A., 2011. Developing an empirical formulae to estimate rainfall intensity in Riyadh region. Journal of King Saud University - Engineering Sciences 23, 81–88. https://doi.org/10.1016/j.jksues.2011.03.003.
Al-Wagdany, 2021. Construction of IDF curves based on NRCS synthetic rainfall hyetographs and daily rainfall records in arid regions. Arab. J. Geosci. 14, 527. https://doi.org/10.1007/s12517-021-06922-w.
Awadallah, A., ElGamal, M., ElMostafa, A., ElBadry, H., 2011. Developing Intensity-Duration-Frequency Curves in Scarce Data Region: An Approach using Regional Analysis and Satellite Data. Engineering 3 (3), 215–226. https://doi.org/10.4236/eng.2011.33025.
Awadallah, A.G., Elsayed, A.Y., Abdelbaky, A.M., 2017. Development of design storm hyetographs in hyper-arid and arid regions: case study of Sultanate of Oman. Arab. J. Geosci. 10 (456). https://doi.org/10.1007/s12517-017-3240-5.
Bell, F.C., 1969. Generalized Rainfall-Duration-Frequency Relationships. Journal of Hydraulic Division, ASCE 95 (1), 311–327.
Bermúdez, M., Cea, L., Uytven, E.V., Willems, P., Farfán, J.F., Puertas, J., 2020. A Robust Method to Update Local River Inundation Maps Using Global Climate Model Output and Weather Typing Based Statistical Downscaling. Water Resources Management 34, 4345–4362. https://doi.org/10.1007/s11269-020-02673-7.
Bernard, M., 1932. Formulas for Rainfall Intensities of Long Duration. Trans. Am. Soc. Civ. Eng. 96, 592–624.
Bracken, C., Holman, K.D., Rajagopalan, B., Moradkhani, H., 2018. A Bayesian Hierarchical Approach to Multivariate Nonstationary Hydrologic Frequency Analysis. Water Resour. Res. 54 (1), 243–255. https://doi.org/10.1002/2017WR020403.
Chen, C., 1983. Rainfall Intensity-Duration-Frequency Formulas. J. Hydraul. Eng. 109 (12), 1603–1621.
Cheng, L., AghaKouchak, A., 2014. Nonstationary precipitation intensity-duration-frequency curves for infrastructure design in a changing climate. Sci. Rep. 4 (7093), 1–6. https://doi.org/10.1038/srep07093.
Chow, V.T., 1953. Frequency analysis of hydrologic data with special application to rainfall intensities. Illinois University of Illinois Engineering Experiment Station, Urbana.
Chow, V.T., Maidment, D.R., Mays, L.W., 1988. Applied hydrology. McGraw-Hill, New York.
Cosgrove, W.J., Loucks, D.P., 2015. Water management: Current and future challenges and research directions. Water Resour. Res. 51, 4823–4839. https://doi.org/10.1002/2014WR016869.
El-Sayed, E.A.H., 2011. Generation of rainfall intensity duration frequency curves for ungauged sites. Nile Water Science & Engineering Journal 4 (1), 112–124. https://doi.org/10.1007/s41748-017-0008-8.
Elsebaie, I.H., 2012. Developing rainfall intensity–duration–frequency relationship for two regions in Saudi Arabia. Journal of King Saud University - Engineering Sciences 24 (2), 131–140. https://doi.org/10.1016/j.jksues.2011.06.001.
FAO, 2021. AQUASTAT Country profile - Oman. Food and Agriculture Organization of United Nation, Rome.
FMO, 2022. Official map of the Sultanate of Oman Retrieved 12 July, 2022, from https://fm.gov.om/ministry/media/downloads/.
Forestieri, A., Arnone, E., Blenkinsop, S., Candela, A., Fowler, H., Noto, L.V., 2018. The impact of climate change on extreme precipitation in Sicily, Italy. Hydrol. Process. 32, 332–348. https://doi.org/10.1002/hyp.11421.
Gumbel, E.J., 1958. Statistics of Extremes. Columbia University Press, New York.
Gunawardhana, L.N., Al-Rawas, G.A., 2016. A Comparison of Trends in Extreme Rainfall Using 20-Year Data in Three Major Cities in Oman. The Journal of Engineering Research 13 (2), 137–148.
Isaaks, E.H., Srivastava, R.M., 1989. An Introduction to Applied Geostatistics. Oxford University Press, New York.
Ishak, E.H., Rahman, A., Westra, S., Sharma, A., Kuczera, G., 2013. Evaluating the non-stationarity of Australian annual maximum flood. J. Hydrol. 494, 134–145. https://doi.org/10.1016/j.jhydrol.2013.04.021.
Kotoub, S., 2004. Design Flood Peaks, Standards, and Wadi Characteristics. Muscat: Japan International Cooperation Agency (JICA), Ministry of Transport. Communication and Information Technology (MTCIT) Sultanate of Oman.
Kotz, S., Nadarajah, S., 2000. Extreme Value Distributions: Theory and Applications. Imperial College Press, London.
Kourtis, I.M., Tsihrintzis, V.A., 2022. Update of intensity-duration-frequency (IDF) curves under climate change: a review. Water Supply 22 (5), 4951. https://doi.org/10.2166/ws.2022.152.
Koutsoyiannis, D., Kozonis, D., Manetas, A., 1998. A mathematical framework for studying rainfall intensity-duration-frequency relationships. J. Hydrol. 206 (1–2), 118–135. https://doi.org/10.1016/S0022-1694(98)00097-3.
Kwarteng, A.Y., Dorvlo, A.S., Kumar, G.T.V., 2009. Analysis of a 27-year rainfall data (1977–2003) in the Sultanate of Oman. Int. J.Of Climatology 29, 605–617.
Li, J.Z., Wang, Y.X., Li, S.F., Hu, R., 2015. A Nonstationary Standardized Precipitation Index incorporating climate indices as covariates. J. Geophys. Res. Atmos. 120 (23), 12082–12095. https://doi.org/10.1002/2015JD023920.
Maidment, D., 1993. Handbook of Hydrology. McGraw-Hill, New York.
Mays, L.W., 2005. Water Resources Engineering. ohn Wiley & Sons, New Jersey.
MRMWR, 2013. Water Balance Computation for the Sultanate of Oman. Ministry of Regional Municipalities and Water Resources, Muscat.
MWR, 1995. Water resources of the Sultanate of Oman an introductory guide. Ministry of Water Resources, Muscat.
Noor, M., Ismail, T., Shahid, S., Asaduzzaman, M., Dewan, A., 2022. Projection of rainfall intensity-duration-frequency curves at ungauged location under climate change scenarios. Sustain. Cities Soc. 83. https://doi.org/10.1016/j.scs.2022.103951.
Ouali, D., Cannon, A.J., 2018. Estimation of rainfall intensity–duration–frequency curves at ungauged locations using quantile regression methods. Stoch. Env. Res. Risk A. 32, 2821–2836. https://doi.org/10.1007/s00477-018-1564-7.
Raiford, J.P., Aziz, N.M., Khan, A.A., Powell, D.N., 2007. Rainfall Depth-Duration-Frequency Relationships for South Carolina, North Carolina, and Georgia. Am. J. Environ. Sci. 3 (2), 78–84. https://doi.org/10.3844/ajessp.2007.78.84.
Roberts, N., Wright, H.E., 1993. Vegetational, lake level, and climatic history of the Near East and Southwest Asia. In: Wright, H.E., Kutzbach, J.E., Webb, T., Ruddiman, W.F., Street-Perrott, F.A., Bartlein, P.J. (Eds.), Global Climates Since the Last Glacial Maximum. University of Minnesota Press, Minneapolis, pp. 194–220.
Sherif, M., Almulla, M., Shettya, A., Chowdhurya, R.K., 2014. Analysis of rainfall, PMP and drought in the United Arab Emirates. Int. J. Climatol. 34, 1318–1328. https://doi.org/10.1002/joc.3768.
Sheskin, D.J., 2000. Handbook of Parametric and Nonparametric Statistical Procedure-. Chapman and Hall/CRC, Boca Raton.
Shrestha, A., Babel, M.S., Weesakul, S., Vojinovic, Z., 2017. Developing intensity-duration-frequency (IDF) curves under climate change uncertainty: the case of Bangkok, Thailand. Water 9 (2), 145. https://doi.org/10.3390/w9020145.
Silva, D.F., Simonovic, S.P., Schardong, A., Goldenfum, J.A., 2021. Assessment of non-stationary IDF curves under a changing climate: Case study of different climatic zones in Canada. J Hydrol. Reg. Stud. 36 (5) https://doi.org/10.1016/j.ejrh.2021.100870.
Uraba, M.B., Gunawardhana, L.N., Al-Rawas, G.A., Baawain, M.S., 2019. A downscaling-disaggregation approach for developing IDF curves in arid regions. Environ. Monit. Assess. 191 (245). https://doi.org/10.1007/s10661-019-7385-4.
Vinnarasi, R., Dhanya, C.T., 2022. Time-varying Intensity-Duration-Frequency relationship through climate-informed covariates. J. Hydrol. 604. https://doi.org/10.1016/j.jhydrol.2021.127178.
Yang, C. S., Kao, S. P., Lee, F. B., and Hung, P. S. 2004. Twelve different interpolation methods: A case study of Surfer 8.0, geo-imagery bridging continents. Paper presented at the XXth ISPRS Congress, Istanbul.
Yu, P.S., Yang, T.C., Lin, C.S., 2004. Regional rainfall intensity formulas based on scaling property of rainfall. J. Hydrol. 295 (1–4), 108–123.